

Laboratori Nazionali di Frascati

LNF-69/51

R. Habel and G. Marangoni : A LENARD-WINDOW IMAGE TUBE FOR
ASTRONOMICAL USE

Estratto da : Jnl. Sci. Instr. (Jnl. Phys. E), 2, 751 (1969)

A Lenard-window image tube for astronomical use

R Habel and G Marangoni

Laboratori Nazionali del CNEN, Frascati, Italy

MS received 24 June 1968, in revised form 6 May 1969

Abstract The construction of a Lenard-window image tube is described and the results obtained are given. The resolving power measured is 80 line pairs per mm on Ilford G5 nuclear emulsion and the speed gain obtained is 10 with respect to a Kodak 103a-0 photographic emulsion. The image shift, due to the static distribution of electric charges on the tube walls, is avoided by the particular construction technique.

1 Introduction

Results are reported which were obtained in the study and development of an electronographic image tube for astronomical use. The tube has a front-faced Cs_3SbO cathode and a mica window with a useful area of $5\text{ mm} \times 27\text{ mm}$; it can be operated up to 40 kv and can be used for exposures up to one hour. The resolving power obtained is 80 lines pairs per mm.

2 Tube construction

The principle of operation of image tubes is well known (McGee and Wheeler 1962). The optical image which is focused on to the photocathode generates an electron image which is accelerated and focused by the action of both an electric and a magnetic field. The electrons then pass through a thin Lenard window and the image is recorded directly on a nuclear emulsion.

An image tube has been constructed by sealing together alternate rings of kovar and glass by induction heating. This

structure which was also used in the construction of multi-stage cascaded image intensifiers (Habel *et al.* 1966), allows a high precision both in the spacing and the aligning of electrodes. This results in a very uniform electric field. The kovar rings (figure 1) are spaced 1 cm apart over the full length of the tube (30 cm). Their inner diameter is 33 mm while the diameter of the glass rings is 58 mm. This arrangement results in a reduction of the background which is due to electron multiplication along the glass wall. The electric field distortion due to the charges on the walls is also avoided.

The kovar rings are blackened electrolytically to avoid the backward scattering of light. The medium softening point glass (Schott No. 8482) which was used could be outgassed during evacuation at temperatures up to 350°C .

The gas desorption during the pinch-off was negligible and in any case does not cause any reduction in the cathode efficiency.

3 The mica window

The mica window, $4\ \mu\text{m}$ thick, was sealed with a low melting point glass solder to a slotted titanium plate 1 mm thick, 22 mm high, 45 mm wide, which is brazed on to the kovar end-plate (figure 2). The glass used for this purpose is made by melting a mixture of PbO , B_2O_3 , SiO_2 in a platinum crucible; the batch composition was: PbO , 72%; B_2O_3 , 14%; SiO_2 , 14%. The glass obtained was ball-milled into powder of 0.10–0.16 mm mesh, which was applied with ethyl alcohol.

The glass-alcohol mixture was first brushed on to the external front of the titanium sheet, then fired at 590°C . To prevent oxidation, the uncovered parts of titanium were painted with colloidal platinum paint (figure 2). The mica sheet was then supported on the titanium plate, its edges were carefully covered with glass-alcohol mixture and the seal was made at a temperature of 540°C , which is the minimum temperature for the glass used. At higher temperatures the strength of the window decreases.

The useful window area is $5\text{ mm} \times 27\text{ mm}$. The slight

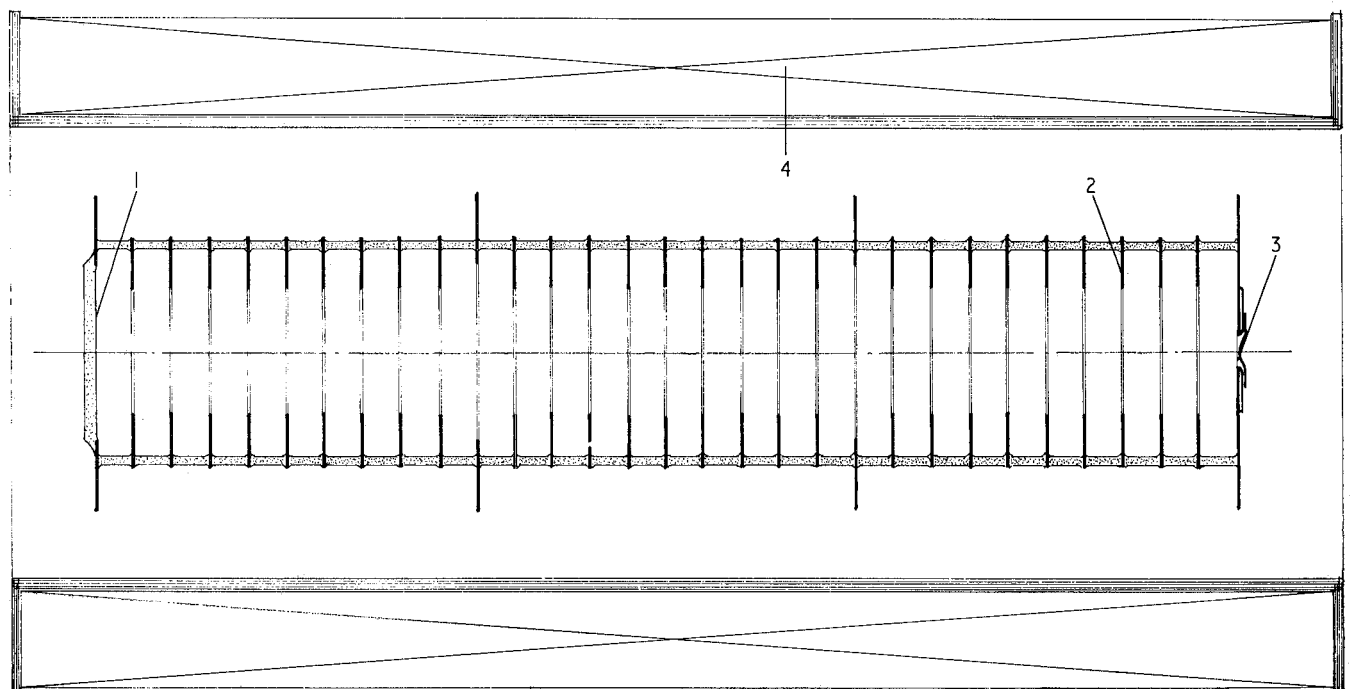


Figure 1 Mica window tube: 1, photocathode; 2, electrical accelerating system (kovar rings); 3, mica window; 4, focusing coil

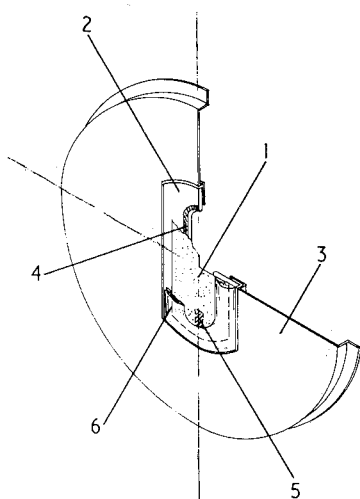


Figure 2 Exit window: 1, mica sheet; 2, titanium slab; 3, kovar plate; 4, uncovered parts of titanium; 5, strips of platinum painted on to the mica; 6, solder glass

difference in the expansion coefficients between titanium and mica causes a pre-stretching of the mica sheet.

The inner front of the mica window was metalized by evaporation of aluminium under high vacuum to a thickness of about 600 Å. This surface then was blackened by aluminium evaporation under an argon atmosphere at a pressure of 2–3 torr. Two stripes of platinum were painted on to the mica sheet (figure 2) to ensure electrical contact between the

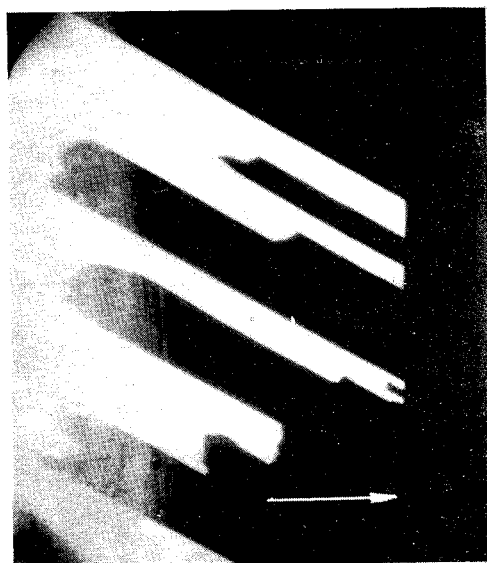


Figure 3 Rupture edge of the mica. The arrow shows the direction of the slow axis

metalization and the metal flange when the mica was pressed against the titanium. The window assembly is joined to the tube by argon-arc welding.

The first windows that were constructed with this technique showed large fluctuations in the rupture load, starting at values as low as 1 kg cm⁻². It was found that the higher values were associated with particular orientation of the rupture edge of the mica (figure 3), which was along to the 'slow optical axis' parallel to the length of the window.

A set of tests was made to study possible mechanical anisotropy of the mica corresponding to the optical one.

Each test consisted of tearing two specimens cut out from the same mica sheet with the tearing direction parallel to the slow and fast axis. The approximate specimen dimensions were 5 μm thick, 20 mm wide, 25 mm long. In figure 4 the

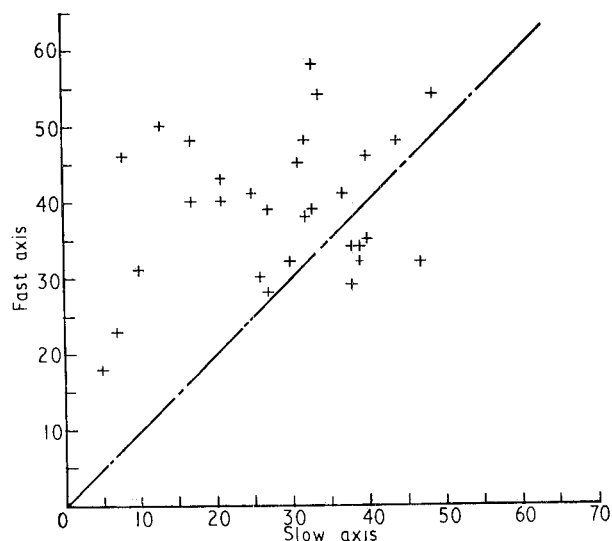


Figure 4 Plot of the results of tearing tests on mica sheets

results obtained from 30 tearing tests are shown. Quantities are plotted proportional to the maximum tensile stress in the two tearing directions (along the slow and fast axes). Each point represents the result of the test on a single mica sheet. The asymmetry of the distribution of points in the slow axis–fast axis plane seems to confirm the existence of the anisotropy.

From this graph the average value for the ratio $\rho = S_f/S_s$ of the stresses along the two tearing directions is 1.66 and the most probable value is 1.21.

The results were obtained in a quite rough way; nevertheless the mica windows that were produced taking in to account this anisotropy show a more regular behaviour, and the lower rupture limit is increased to approximately 4 kg cm⁻² for window of area 7 mm × 30 mm.

4 Photocathode formation

The photocathode is processed directly inside the tube on the front window, without a processing chamber. The tube is thoroughly evacuated to a pressure of 1–3 ntorr.

The antimony layer is obtained by evaporation with a molecular gun (figure 5). The antimony powder is held in a quartz tube of 2 mm outside diameter, 1 mm inside diameter which also contains the heater coil made of tungsten wire. The antimony vapour emerges from a hole in the thinned cylindrical wall of the tubing. The hole diameter is 0.1 mm and the wall thickness is about the same. The antimony beam emerging is baffled to cover (at the distance of 8 cm) the whole cathode area.

The antimony thickness is measured by white light absorption and the evaporation is terminated at a light absorption of 25%. The caesium vapour is then introduced at 150°C until the sensitivity of the cathode has decreased by a few per cent from the maximum value. The caesium inlet is then closed and the temperature lowered to about 130°C until the sensitivity reaches the maximum value.

After activation of the cathode, the tube is cooled and the cathode oxidized; the oxygen (spectroscopic grade) is introduced into the vacuum system from a glass bottle at atmospheric pressure through an adjustable leak. The leak rate is regulated to increase the pressure to about 10 ntorr.

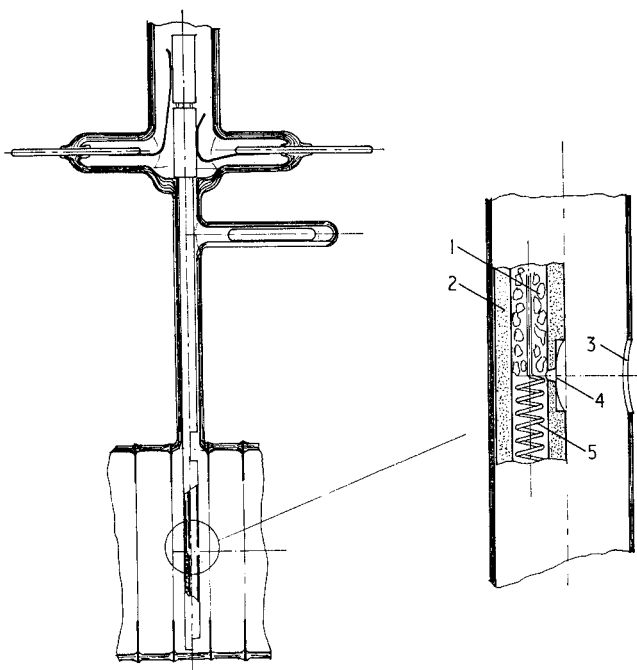


Figure 5 Molecular gun: 1, antimony; 2, quartz tubing; 3, baffling hole; 4, exit hole; 5, heater

During this operation the cathode sensitivity is monitored, and just before the sensitivity has reached its maximum value the oxygen flow is cut-off.

5 Tube operation

The magnetic field is obtained from a solenoid powered by a current stabilizer with a long-term stabilization of 10^{-3} . The high voltage to the tube is also stabilized to 10^{-3} . With a high voltage of 40 kv and an axial magnetic field of the order of 140 G the electron optical image is formed on the mica window after two complete spirals.

The image is recorded on a photographic emulsion (Ilford G5, 10 μm thick, on a Melinex support) which is pressed against the mica window by means of a thin rubber membrane. The required pressure of about 0.2 atm is obtained by compressed air. Under these working conditions the resolving power over the full length of the window, measured with a Baum (1962) test pattern is 80 lines pairs per mm (figure 6).

In figure 7 a photograph of a square grid pattern test is shown. The measured value of the coefficient C_x of spiral distortion, which is defined as the ratio of the incremental rotation $\Delta\psi$ of the image point to the square of the distance r from axis, is $\Delta\psi/r^2 = 3.3 \times 10^{-4} \text{ rad mm}^{-2}$.

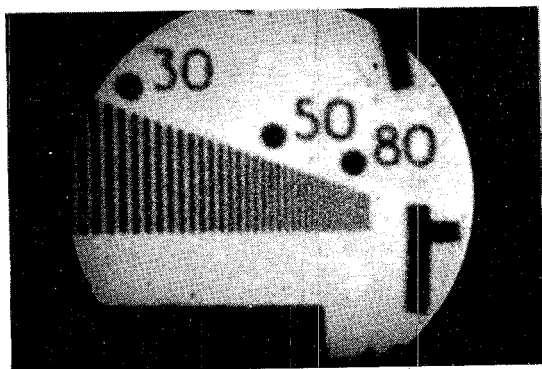


Figure 6 Enlarged view of a resolution test showing the resolving power of the tube

No shift of the image was observed even during the first minutes of operation. Two exposures taken at interval of 15 minutes (the first was taken one minute after switching on) were found to overlap within 80 lines pairs per mm.

Although the photocathode is formed directly inside the tube envelope, the background is satisfactorily low. With exposures of one hour at room temperature a density of 0.2 is obtained.

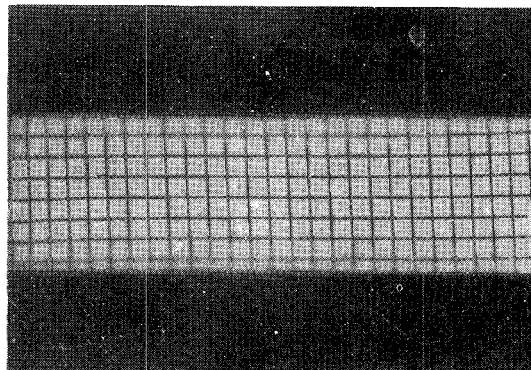


Figure 7 Square grid-pattern distortion test. This picture was taken on a 35 mm Kodak microfilm; due to the thickness of the film the contact against the mica window was poor at the upper and lower edges

The speed of the tube has been measured with reference to Kodak 103a-0 plates. For this purpose a circular disk of light at a wavelength of 4350 \AA was focused either directly on the 103a-0 or on to the photocathode of the tube. The electron image was recorded on the Ilford G5. The accelerating voltage of the tube was 40 kv. The light intensity was chosen to allow exposures of up to one hour.

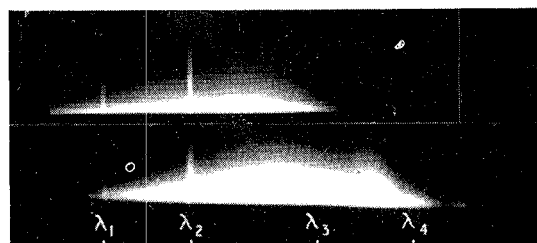


Figure 8 Spectral sensitivities of: (a) Kodak 103a-0; (b) photocathode. $\lambda_1 = 4046.56 \text{ \AA}$; $\lambda_2 = 4358.35 \text{ \AA}$; $\lambda_3 = 5000 \text{ \AA}$; $\lambda_4 = 6000 \text{ \AA}$

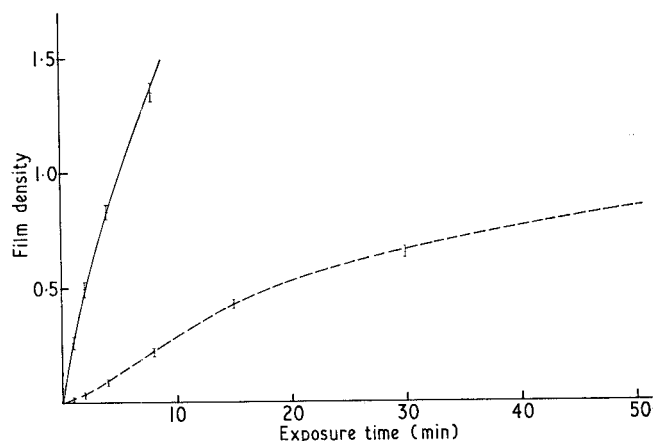


Figure 9 Recorded density as a function of the exposure time

Notes on experimental technique and apparatus

The spectral sensitivities of the 103a-0 and tube photocathode are shown in figure 8; figure 9 is a plot of the film density (above the fog) against exposure time for the Ilford G5 emulsion (solid line) and for Kodak 103a-0 (broken line). The results given here were obtained from measurements on a tube with low cathode sensitivity ($15 \mu\text{A lm}^{-1}$); more recent tubes have sensitivities in the range of $30\text{--}40 \mu\text{A lm}^{-1}$.

An interesting feature of our tubes is their life; after one year we have measured no appreciable lowering of the photocathode sensitivity and no increase in background.

Work is in progress to apply the same techniques in the fabrication of tubes with an S.20 photocathode.

References

Baum W A 1962 *Adv. Elect. Electron Phys.* **16** 391–401

Habel R Letardi T and Marangoni G 1966 *Alta Freq.* **35** 197–201

McGee J D and Wheeler B E 1962 *Adv. Elect. Electron Phys.* **16** pp. 47–59

McGee J D Khogali A and Ganson A 1966 *Adv. Elect. Electron Phys.* **22A** 11–30